

# Polyamide-Montmorillonite Nanocomposites as a Drug Delivery System: Preparation, Release of 1,3,4-Oxa(thia)diazoles, and Antimicrobial Activity

Nehal Salahuddin,<sup>1</sup> Ahmed Elbarbary,<sup>1</sup> Nanis G. Allam,<sup>2</sup> Ayat F. Hashim<sup>3</sup>

<sup>1</sup>Department of Chemistry, Faculty of Science, Tanta University, Tanta 31527, Egypt

<sup>2</sup>Department of Botany, Faculty of Science, Tanta University, Tanta 31527, Egypt

<sup>3</sup>Plant Pathology Research Institute, Agricultural Research Center, Giza, Egypt

Correspondence to: N. Salahuddin (E-mail: salahuddin.nehal@yahoo.com)

**ABSTRACT:** New microbicidal polyamides were prepared by the reaction of 5-phenyl-1,3,4-oxadiazole-2-thiol, 5-phenyl-1,3,4-oxadiazole-2-amine, and 5-(4-chlorophenyl)-1,3,4-thiadiazole-2-thiol with ethyl chloroformate followed by polycondensation with polyoxypropylenetriamine (Jeffamine T<sub>403</sub>). The polyamides were modified to yield amine hydrochloride. The intercalation of polyamides into montmorillonite (MMT) was achieved through an ion exchange process between sodium cations in MMT and amine hydrochloride in the polyamides. The structure of the resulting materials was characterized with elemental analysis, proton nuclear magnetic resonance, Fourier transform infrared-spectroscopy, X-ray diffraction, thermogravimetric analysis, and transmission electron microscope. The release behavior of 1,3,4-oxa(thia)diazoles was investigated in buffered aqueous solution at different pH values (2.3, 5.8, and 7.4). A slow release was recorded from the nanocomposites whereas; the release reaches almost 90% from polyamides. The *in vitro* antimicrobial activity of the polyamides and nanocomposites was studied against Gram-negative bacteria, Gram-positive bacteria, Yeast and the filamentous fungi by well diffusion method. The polymers showed good or moderate antimicrobial activities. However, nanocomposites showed no antimicrobial effect. Furthermore, *in vivo* study showed that nanocomposites had good antimicrobial activity. © 2014 Wiley Periodicals, Inc. *J. Appl. Polym. Sci.* **2014**, *131*, 41177.

**KEYWORDS:** clay; drug delivery systems; nanocomposites; polyamides

Received 9 February 2014; accepted 16 June 2014

DOI: 10.1002/app.41177

## INTRODUCTION

1,3,4-Oxa(thia)diazoles derivatives exhibit a wide range of biological activities including antibacterial,<sup>1</sup> antitubercular,<sup>2</sup> vasodilatory,<sup>3</sup> antifungal,<sup>4</sup> cytotoxic,<sup>5</sup> anti-inflammatory and analgesic,<sup>6,7</sup> hypolipidemic,<sup>8</sup> anticancer,<sup>9</sup> and ulcerogenic activities.<sup>10</sup>

A variety of polymers have been used for medical care including preventing medicine, clinical inspections, and surgical treatments of diseases.<sup>11,12</sup> Numerous polymer biomaterials have been employed for such medical purposes because they have acceptable biocompatibility, biodegradability, and absorbability.<sup>13</sup> These polymer materials can act as drug carriers by controlling the release rate of drug initially loaded in application for drug delivery systems.<sup>14</sup> Delivery of drugs dosage for optimal lengths of time will make them more effective and more powerful. Aliphatic polyamide microcapsules were synthesized by the process of interfacial polymerization.<sup>15</sup> This system showed the potential to

liberate the incorporated model drug effectively by the process of diffusion through the polyamide microcapsule membrane. Self-regulating reservoir system was prepared with hydrophilic aliphatic polyamide microcapsules containing succinylamidophenyl glucopyranoside insulin (SAPG-insulin) and cross linked concanavalin A (Con A) enclosed in a pouch polymeric membrane. The *in vitro* data demonstrated rapid diffusion of both glucose and SAPG-insulin across the microcapsule membrane with a short lag time for exchange.<sup>16</sup> The efficiency of the hollow polyamide fibers in releasing glycerin trinitrate in order to reduce blood pressure with minimal dermal toxicity was explored. The results showed that the quantity of glycerin trinitrate released per minute within the polyamide hollow fibers was sufficient to reduce blood pressure significantly while it did not show considerable dermal toxicity.<sup>17</sup>

Montmorillonite clay mineral (Na-MMT) is one of the smectite group, composed of an alumina octahedral sheet sandwiched

Additional Supporting Information may be found in the online version of this article.

© 2014 Wiley Periodicals, Inc.

between two tetrahedral silica sheets. The imperfection of the crystal lattice and isomorphous substitution induce a net negative charge that leads to the adsorption of alkaline earth metal ions in the interlayer space. Such imperfection is responsible for the activity and exchange reactions with organic compounds. Smectite clays intercalated by drug molecules have attracted great interest from researchers since they exhibit novel physical and chemical properties.<sup>18–20</sup> Lin et al.<sup>21</sup> studied the intercalation of 5-fluorouracil with MMT as drug carrier. Zheng et al.<sup>22</sup> have investigated the intercalation of ibuprofen into MMT as sustained release drug carrier. Fejer et al.<sup>23</sup> studied the intercalation and release behavior of promethazine chloride and bufornin hydrochloride from MMT. Several minerals with layer structure have been used as antimicrobial carriers.<sup>24–26</sup> However, despite the beneficial effect of clay, there are some inherent drawbacks associated with the use of clay for drug delivery. Under physiological conditions clay dispersions are unstable and tend to flocculate and precipitate in ion containing solutions. In this regard, it is believed that the synthesis of polymer nanocomposites would alleviate this disadvantage by exploiting the properties of clay and polymer in such a way that the behavior of the clay is modified.

Polymer nanocomposites based on nano-layered silicate have attracted much attention during the past years because of their low cost, their ready availability and their non-isometric structure derived from high aspect ratio, which can maximize the reinforcing effect in terms of mechanical, thermal and barrier properties.<sup>27–32</sup> Lee et al.<sup>33</sup> investigated the effect of MMT on physical properties of poly *N*-isopropylacrylamide/MMT nanocomposites hydrogel and drug release behavior. Meng et al.<sup>34</sup> studied the antimicrobial activity of polydimethylsiloxane/MMT-Chlorohexidine acetate nanocomposites.

Recently, we studied the release of ibuprofen and theophylline from clay modified by polyoxypropylenediamine. These nanocomposites were expected to achieve *in situ* release for colon rectal therapy.<sup>35</sup> In addition, the bioactive agents, vanillin,<sup>36</sup> *P*-hydroxymethylbenzoate, 2,4-dihydroxymethyl benzoate, and methyl salicylate<sup>37</sup> incorporated into polyoxypropylenediamine were tested for their antimicrobial activities. The inhibition effect depends on molecular weight of polymer and morphology of the resulting nanocomposites. The release of 5-amino salicylic<sup>38</sup> acid from chitosan-layered silicate nanocomposites was studied. The dispersed layered silicate platelets encase the 5-ASA retarding the release of drug molecule in the nanocomposites. Chitosan polytetrahydrofuran-MMT nanocomposite showed strong antimicrobial activity<sup>39</sup> particularly against gram-positive bacteria. However, Na-MMT could not inhibit the growth of bacteria.

In this study, 1,3,4-oxa(thia)diazoles were loaded into polyamide via the reaction of 5-phenyl-1,3,4-oxadiazole-2-thiol, 5-phenyl-1,3,4-oxadiazole-2-amine, and 5-(4-chlorophenyl)-1,3,4-thiadiazole-2-thiol with ethyl chloroformate followed by polycondensation with polyoxypropylenetriamine. Then, the polyamides were modified to yield amine hydrochloride followed by intercalation of the polymers into montmorillonite through an ion exchange process between sodium cations in Na-MMT and  $\text{NH}_3^+$  groups in the polymer. Release of 1,3,4-oxa(thia)diazoles

from polyamide nanocomposites was studied. In addition, the antimicrobial activities of polyamide and nanocomposites against Gram-negative and Gram-positive bacteria, yeast, and filaments fungi were investigated. Furthermore, antimicrobial, toxicity and anti-inflammatory properties in experimental animals of tested compounds was evaluated. To our knowledge, this is the first study which has shown the antimicrobial effect of nanocomposites based on polyamide layered silicates loaded with diazoles.

## MATERIALS AND METHODS

### Materials

The clay mineral used in this study was sodium montmorillonite (Na-MMT; colloid Bp) from southern Clay Products Inc (Gonzales, TX) with cation exchange capacity (CEC) of 114.8 meq/100 g. Polyoxypropylenetriamine (Jeffamine T<sub>403</sub>) was obtained from Huntsman Corporation (TX) having a trifunctional primary amine, an average molecular weight of approximately 440. Its amine groups are located on secondary carbon atoms at the ends of aliphatic polyether chains. Its viscosity at 25 °C is 70 cst; 1,4-Dioxane and dimethyl sulfoxide (DMSO) were purchased from Sigma-Aldrich. Ethyl chloroformate was purchased from Fluka Company. Ethanol, methanol, and dimethyl formamide (DMF) were purchased from El Nasr Pharmaceutical Chemicals, Egypt.

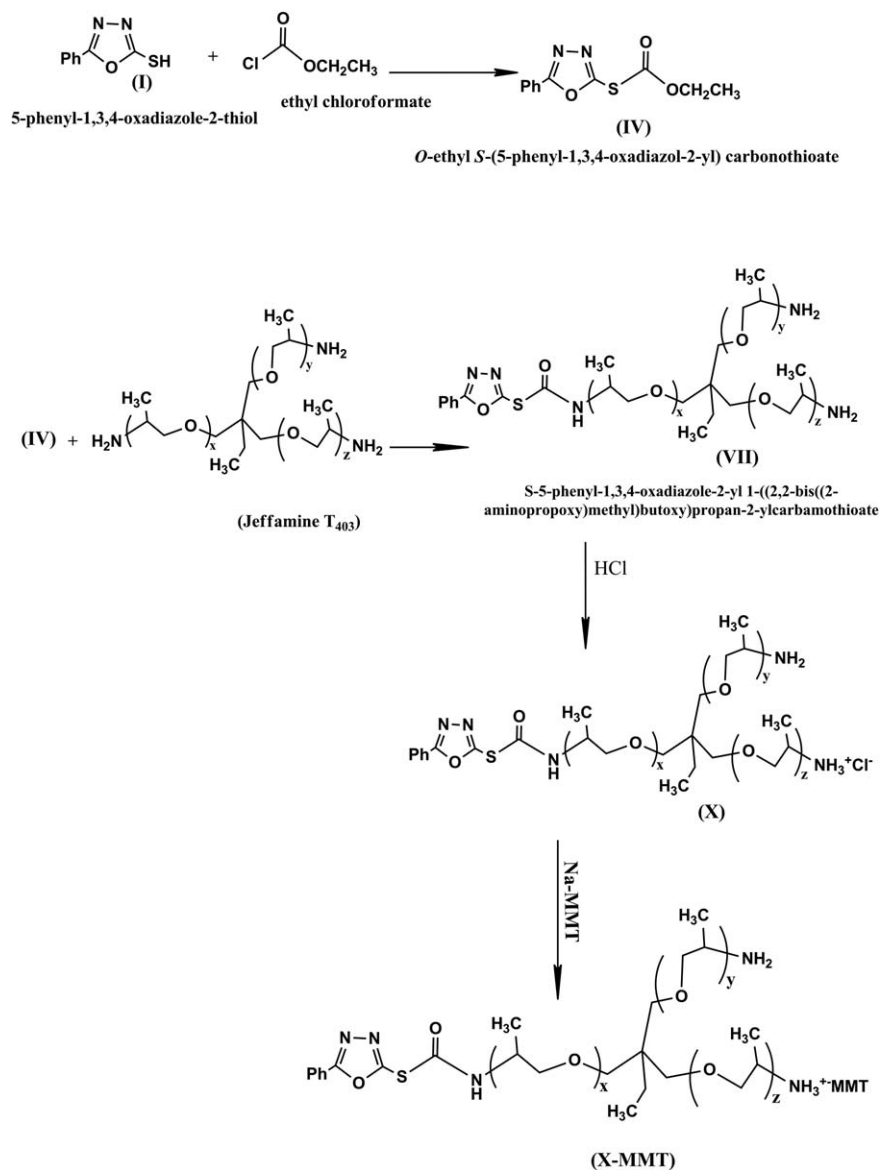
### Preparation of Polyamide-MMT Nanocomposites (X-MMT, XI-MMT, XII-MMT)

1,3,4-Oxa(thia)diazole derivatives were prepared according to the recommended methods.<sup>40–42</sup>

**Preparation of 5-Phenyl-1,3,4-oxadiazole-2-thiol (I).** Benzoic hydrazide (1.36 g, 0.01 mol) was refluxed with carbon disulfide (0.76 g, 0.01 mol) and potassium hydroxide (0.56 g, 0.01 mol) in ethanol (100 mL) for 4 hr and followed by thin layer chromatography (TLC) until the starting material was consumed. The reaction mixture was concentrated and cooled. The residual solid was dissolved in water (200 mL), neutralized with 15% HCl (10 mL). The precipitate was filtered off, washed with water, dried and recrystallized from ethanol, to give I, 1.02 g, 78% yield, melting point (m.p.) 219°C.<sup>40</sup>

**Preparation of 5-Phenyl-1,3,4-oxadiazole-2-amine (II).** A mixture of bromine (8.0 g, 0.1 mol), potassium cyanide (5.0 g, 0.1 mol), and water (20 mL) was added to a solution of benzoic hydrazide (13.6 g, 0.1 mol) and sodium bicarbonate (8.4 g, 0.1 mol) in water (20 mL). The reaction mixture was stirred at 30°C for 2 hr and followed by TLC. The separated solid was filtered off, dried and recrystallized from ethanol, to yield II, 7.2 g, 53% yield, m.p. 240°C.<sup>41</sup>

**Preparation of 5-(4-Chlorophenyl)-1,3,4-thiadiazole-2-thiol (III).** To a solution of 4-chlorobenzoic hydrazide (2.2 g, 0.01 mol) in water (10 mL), concentrated HCl (38%, 2 mL), and potassium thiocyanate (0.97 g, 0.01 mol) was added. The reaction mixture was refluxed for 3 hr and followed by TLC. The white solid formed was filtered off, dissolved in concentrated H<sub>2</sub>SO<sub>4</sub> (95%, 10 mL) and warmed at 50°C for 1 hr. The reaction mixture was cooled, poured into cold water (50 mL) and neutralized with KOH solution (20%, 15 mL). The solid



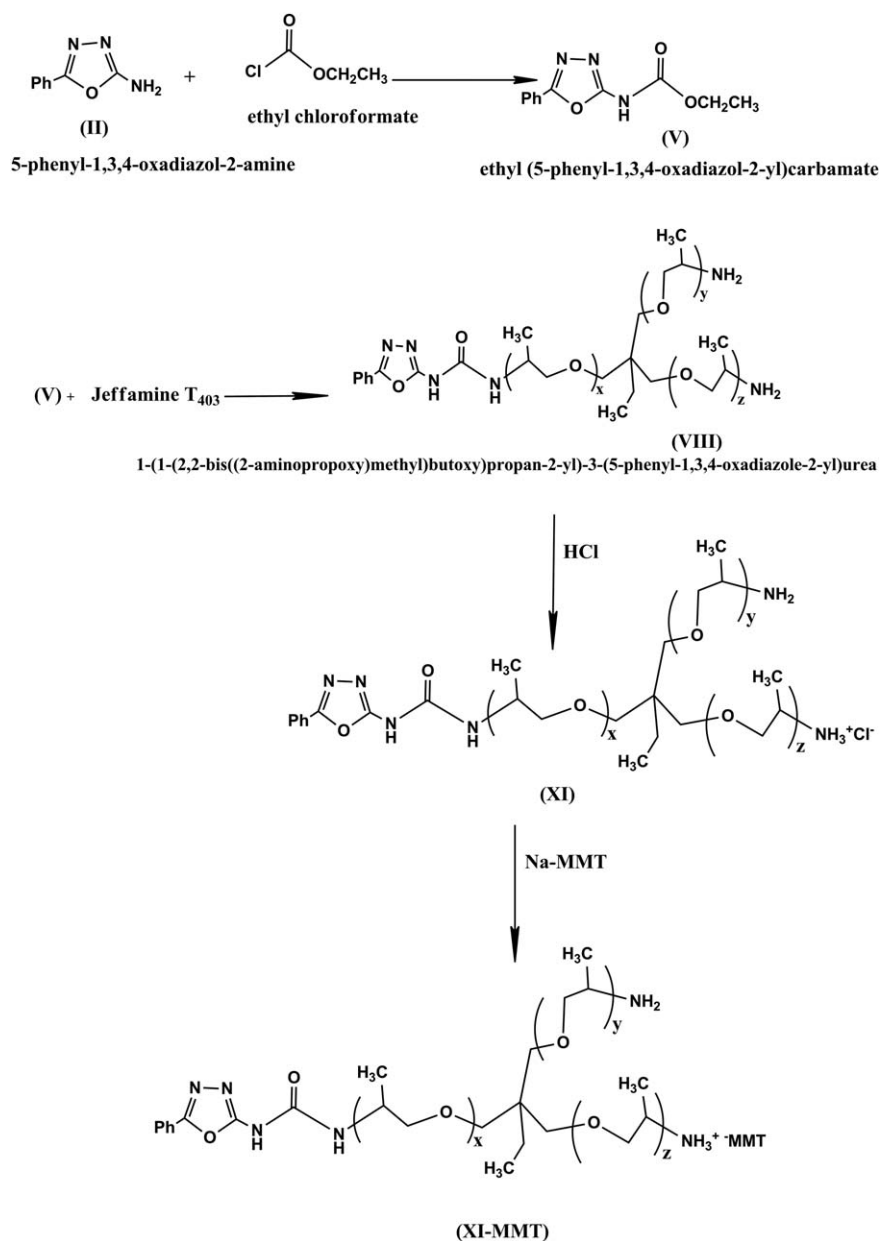
**Scheme 1.** (a–c) Preparation of polyamide-MMT nanocomposites.

product was filtered off, washed with water, dried, and recrystallized from ethanol, to afford **III**, 0.89 g, 65% yield, m.p. 223°C.<sup>42</sup>

**Reaction of Ethyl Chloroformate with 1,3,4-Oxa(thia)diazoles (I, II, and III).** A mixture of **I** (1.0 g, 0.0056 mol) and ethyl chloroformate (0.6 g, 0.0056 mol) was refluxed in 1,4-dioxane (20 mL) for 5 hr and the reaction was followed by TLC. The solvent was evaporated and the solid left was collected and recrystallized from EtOH to afford **IV** (1.58 g, 0.0063 mol, m.p. 132°C).<sup>43</sup> The same procedure was done using **II**, **III** to afford **V** (0.4 g, 0.0017 mol, m.p. 205°C),<sup>44</sup> **VI** (0.28 g, 0.0077 mol, m.p. 220°C) respectively.

**Preparation of Polyamides (VII, VIII, and IX).** Polyamides were prepared by condensation reaction of **IV**, **V**, and **VI** with Jeffamine T<sub>403</sub>. Accordingly, To **IV** (2 g, 0.008 mol) in 100 mL round bottom flask, JeffamineT<sub>403</sub> (1.6 g, 0.003 mol) was added. The mixture was stirred at 30°C for 4 hr. The product (**VII**) was filtered off, washed with 1,4-dioxane (20 mL) and dried in

vacuum oven at 60°C to give 2.3 g as indicated in Scheme 1(a). <sup>1</sup>H-NMR spectrum (Supporting Information Figure S1) of **VII** (300 MHz, DMSO, δ<sub>6</sub>) showed the following signals: 2.49 (t,3H,CH<sub>3</sub>CH<sub>2</sub>), 2.51 (d,3H,CH<sub>3</sub>CH<sub>2</sub>), 4.44 (q,1H,CH<sub>3</sub>CHNH<sub>2</sub>), 4.52 (s,2H,OCH<sub>2</sub>), 4.26 (q,1H,CHCH<sub>3</sub>), 5.12 (s,2H,NH<sub>2</sub>), 12.50 (s,1H,NH) and the aromatic protons (5H) appeared as a multiplet in the range from 7.49 to 7.93 ppm. Elemental analysis: calculated for C<sub>12</sub>H<sub>12</sub>N<sub>3</sub>O<sub>3</sub>S (278.3) S = 5.27%, Found S = 5.29%. The same procedure was done using **V** (1.0 g, 0.0062 mol), Jeffamine T<sub>403</sub> (1.38 g, 0.003 mol) and **VI** (1.5 g, 0.006 mol), Jeffamine T<sub>403</sub> (2.01 g, 0.004 mol) to give **VIII** and **IX**, respectively as shown in Scheme 1(b,c). <sup>1</sup>H-NMR spectrum (Supporting Information Figure S2) of **VIII** (300 MHz, DMSO,δ<sub>6</sub>) confirmed the proposed structure and showed the following signals: 1.002 (t,3H,CH<sub>3</sub>CH<sub>2</sub>), 1.13 (t,3H,CH<sub>3</sub>CH<sub>2</sub>), 1.17 (t,3H,CH<sub>3</sub>CH<sub>2</sub>), 3.02 (t,1H, OCH), 3.39 (t,1H, OCH), 3.12 (t,1H, OCH), 4.07 (s,2H,NH<sub>2</sub>), 7.47 (s,1H,NH),8.50 (s,1H,NH)



Scheme 1. Continued.

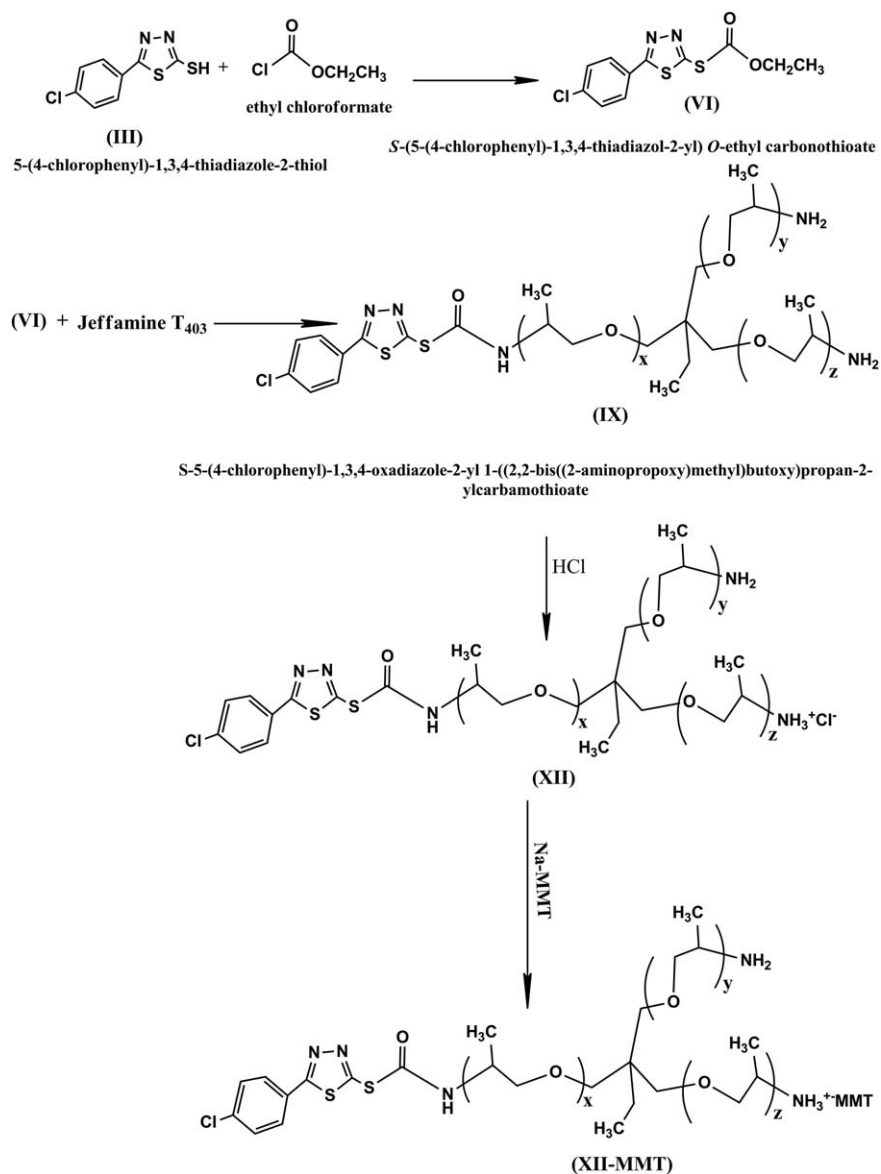
and the aromatic protons (5H) appeared as a multiplet in the range from 7.47 to 7.87 ppm. Elemental analysis: calculated for  $C_{12}H_{13}N_4O_3$  (261.26) N = 7.27%, Found N = 7.25%.  $^1\text{H}$ NMR spectrum (Supporting Information Figure S3) of IX (300 MHz,  $\text{DMSO-d}_6$ ) showed the following signals: 1.07(t,3H, $\text{CH}_3\text{—CH}_2$ ), 1.21(s,3H, $\text{CH}_3$ ), (d,3H, $\text{CH}_3$ ), 2.87(q,1H, $\text{H}_3\text{C—CH}(\text{OCH}_2)\text{NH}_2$ ), 3.35 (d,2H, $\text{OCH}_2\text{—CH}(\text{NH})\text{CH}_3$ ), 4.26 (q,1H, $\text{CH—CH}_2\text{O}$ ), (s,2H, $\text{NH}_2$ ) and the aromatic protons (4H) appeared as a multiplet in the range from 7.58 to 7.97 ppm. Elemental analysis: calculated for  $C_{12}H_{11}N_3ClO_2S_2$  (328.8) S = 9.67 %, Found S = 9.70%.

**Preparation of Polyamide-MMT Nanocomposites (X-MMT, XI-MMT, XII-MMT).** The general idea underlying the preparation of polyamide montmorillonite nanocomposites follows the simple rule of ion exchange process. Accordingly, Na-MMT

(1.0 g) was suspended in distilled water (50 mL), stirred overnight at 25°C followed by addition 1,4-dioxane (30 mL). To VII (1.7 g, 0.006 mol) dissolved in 1,4-dioxane (30 mL) hydrochloric acid was added and the pH was adjusted to be 2.8. The resulting polyamide amine hydrochloride (X) was added portion wise to the above suspension within 1 hr. The white precipitate formed was filtered off, washed several times with water until no chloride ions were detected in the filtrate to afford X-MMT (0.6 g, 60% yield). The same procedure was done using VIII (1.6 g, 0.0015 mol) and IX (1.7 g, 0.005 mol) to give XI-MMT (0.7 g, 70% yield) and XII-MMT (0.6 g, 60% yield) respectively as shown in Scheme 1.

#### Characterization

FT-IR spectra were recorded on Bruker, Tensor 27FT-IR spectrophotometer with frequency range  $4000\text{ cm}^{-1}$  to  $400\text{ cm}^{-1}$



Scheme 1. Continued.

(Central Lab. Tanta University, Egypt). The XRD analysis was measured by GRN,APD 2000 PRO X-ray diffraction, using Cu K $\alpha$  (1.54 Å) at 40 Ku. TGA data were obtained by using Shimadzu thermal analyzer system at a heating rate of 10°C/min, sample weight of 5 to 6 mg, under nitrogen (20 mL/min) flow. The range investigated from 25°C to 800°C. TGA-50 furnace with a M3 microbalance, and TA72 Graphware software were used for thermal analyses (Ain Shams University, Cairo, Egypt). Elemental analysis was determined on Heraeus (micro analysis center, Cairo University, Egypt). <sup>1</sup>HNMR spectra were measured on a Varian Mercury VX-300 (300 MHz) NMR spectrometer (micro analysis center, Cairo University, Egypt). TEM micrographs were taken with a JEOL JEM-1230 electron microscope at an accelerating voltage of 100 KV; 0.1 g of the samples was dispersed in 10 mL acetone using ultra sonic (Clifton ultra 8050-H) and a drop of the suspension was placed on the copper grid for TEM examination (Faculty of Medicine, Tanta Univer-

sity, Egypt). UV-VIS absorption spectra were measured using Shimadzu UV-2101 Dc spectrophotometer.

### Drug Release

**Preparation of Buffer Solutions.** Phosphate buffer solution (PB) were prepared by dissolving sodium phosphate dibasic (21.7 g) and potassium phosphate monobasic (2.6 g) in 1 L deionized water and pH was adjusted to 2.3, 5.8, and 7.4 using 0.1N hydrochloric acid or 0.1N sodium hydroxide, respectively.

**Release Measurements.** Ten milligrams of samples were suspended in 100 mL of PB at pH 2.3, pH 5.8, and pH 7.4. The amount of drug released was determined using UV spectrophotometer at  $\lambda_{\text{max}} = 343$  nm for I;  $\lambda_{\text{max}} = 301$  nm for II; and  $\lambda_{\text{max}} = 248$  nm for III. At specific intervals, 3 mL of the buffer was collected for analysis and each experiment was carried out in triplicate.



### **In Vitro Antimicrobial Activity**

**Test Microorganisms.** The microbial strains were obtained from Bacteriological laboratory of Botany department, Microbiology section, Faculty of science, Tanta University. The Gram-negative bacteria (*Escherichia coli* ATCC 8739, *Aeromonas hydrophila*, *Shigella* sp.), Gram-positive bacteria (*Staphylococcus aureus*, *B. subtilis* ATCC 6633), yeast (*C. albicans*) and the filamentous fungi (*Aspergillus niger*) were used to examine the antimicrobial activity of the polyamides and their nanocomposites. The bacterial strains were maintained on nutrient agar (3 g peptone; 5 g NaCl; 5 g beef extract; 20 g agar per liter, pH = 7.4), while the fungi and yeast were maintained on sabouraud agar (10 g peptone; 20 g glucose, pH = 5.4).

**Antimicrobial Activities.** The antimicrobial activity of the tested samples was determined by well diffusion method. Powder test samples (10 mg/mL) were dissolved in DMSO. In case of nanocomposites the samples were dispersed in DMSO. Wells were then created and 50  $\mu$ L of the samples were pipette into each well to detect the most sensitive microorganisms against investigated polymers and nanocomposites. DMSO was used as negative control. The plates were incubated at 37°C for bacteria and yeasts, and at 30°C for fungi after which they were examined for inhibition zones development. A caliper was used to measure the inhibition zones. Three replicates were carried out at least. The inoculum's concentrations were  $6.5 \times 10^5$  CFU for bacteria and  $4.2 \times 10^4$  CFU for fungi. After incubation for 24 hr for bacteria, yeasts, and at 48 hr for fungi, the agar plates were checked for the diameter of inhibition zone. The reaction of the microorganisms with antimicrobial polymers and nanocomposites was determined by the size of the inhibitory zone.

**Minimal Inhibitory Concentrations (MICs).** The most antimicrobial active compounds (VII, IX) were chosen to determine their MIC values against the most sensitive microorganism by tube dilution assay.

**Tube Dilution Assay.** Nutrient broth was used for the tube dilution to determine MICs for tested bacteria. The MIC value of tested compounds was determined using two-fold broth microdilution.<sup>45</sup> One milliliter of sterile media was added to 1 mL of different compound concentrations (100, 50, 25, 12.5, 6.3, 3.2 and 1.6, 0.8, 0.4, and 0.2 mg/1 mL). The tubes were then inoculated with a drop of microbial suspension (25  $\mu$ L) and incubated at 37°C for 24 hr. Tetracycline (100–0.0031 mg/mL) was used as standards antimicrobial drug (positive control). DMSO was used as the negative control. After incubation, certain amount of each tube was spread on agar plates and then incubated for 24 hr, and then the numbers of colonies were counted. The MIC endpoints were detected as the lowest concentration of tested compounds at which the growth of the tested microorganisms was inhibited. The minimum bactericidal concentration (MBC) end points are defined as the lowest concentration of antimicrobial agent that kills >99.9% of the initial bacterial population and detected when no visible growth of bacteria was observed on the agar plates.

### **In Vivo Study**

**Experimental Animals.** Eight Swiss albino male mice (week old, weighing 18–20 g) were obtained from the animal house at National Research Center (NRC), Giza, Egypt.

**Preparation of Bacterial Inoculums.** *S. aureus* was cultured in manitol salt agar and incubated at 37°C for 24 hr according to the reported method.<sup>46</sup> The number of  $10^8$  CFU/mL bacteria (10  $\mu$ L inoculums in phosphate saline (PS) 0.85%) was freshly prepared.

**Burned Wound Model.** A full thickness burn wound infection was established in mice using *S. aureus* via the topical route. Skin was shaved and mice were anaesthetized with ether fumes. A third degree of burn was induced by applying a heated brass bar (10  $\times$  10  $\times$  100 mm<sup>3</sup>) for 45 sec.

**Treatment of Burned Mouse Model Wound Infection.** The burned site was challenged with *S. aureus* after 30 min of burning and then treated topically after 2 hr. The treatment was repeated twice per day (0.10 mg/day).

**Experimental Model.** Mice were randomly divided into seven groups (each group contains nine mice): first group was not treated and serve as negative control, second, third, fourth, fifth, and sixth groups were treated with (Na-MMT, Mebo (reference drug), VII, X-MMT, IX, and XII-MMT) (0.10 mg/day), respectively. The experiment was continued for 6 days. The mice were scarified each 2 days (three mice in each time). Blood and organs (spleens, livers, and the burnt skins) were measured as parameters for efficiency of treatments.

**Bacterial Load in Blood and Organs.** The blood and organs (spleens, livers and the burnt skins) of experimental animals were aseptically collected after dissection to determine the bacterial counts. The blood (200  $\mu$ L) was serially diluted in sterile BS and 30  $\mu$ L of the diluted blood was cultured on manitol salt agar plates for growth. For the tissues, samples were homogenized in 5 mL of sterile BS and serially diluted in sterile BS then, cultured on manitol agar plates. The inoculated plates were overnight incubated at 37°C. The number of colonies that grew on manitol agar plates was counted. Number of bacteria (CFU/organ) = (average number of bacterial colonies/ amount plated)  $\times$  dilution.

**Toxicity of Tested Compounds on Healthy Mice Skin.** Mice were randomly divided into six groups (each group contains six mice): first group was treated with 1,4-dioxane serve as control, second, third, fourth, and fifth groups were treated with Na-MMT, VII, X-MMT, IX, and XII-MMT, respectively. The single patch application test (S-PAT) was conducted to confirm that the tested compounds were not a skin irritant even under highly exaggerated exposure conditions (48 hr).<sup>47</sup> A double gauze layer was applied onto the skin and the patches were covered with a non reactive tape and the entire test site was wrapped with a binder. The test site was observed for signs of irritation (the development of a rash, inflammation, swelling, scaling, and abnormal tissue growth in the affected area) over the next 5 days.

**Statistical Analysis.** One-way analysis of variance (ANOVA) was carried out for obtained results during this study using SPSS. All experiments and analytical determinations were replicated at least three times and mean value was calculated. Fisher (*F*) and probability (*P*) values were calculated.

*F* = Variance between groups/variance within groups.

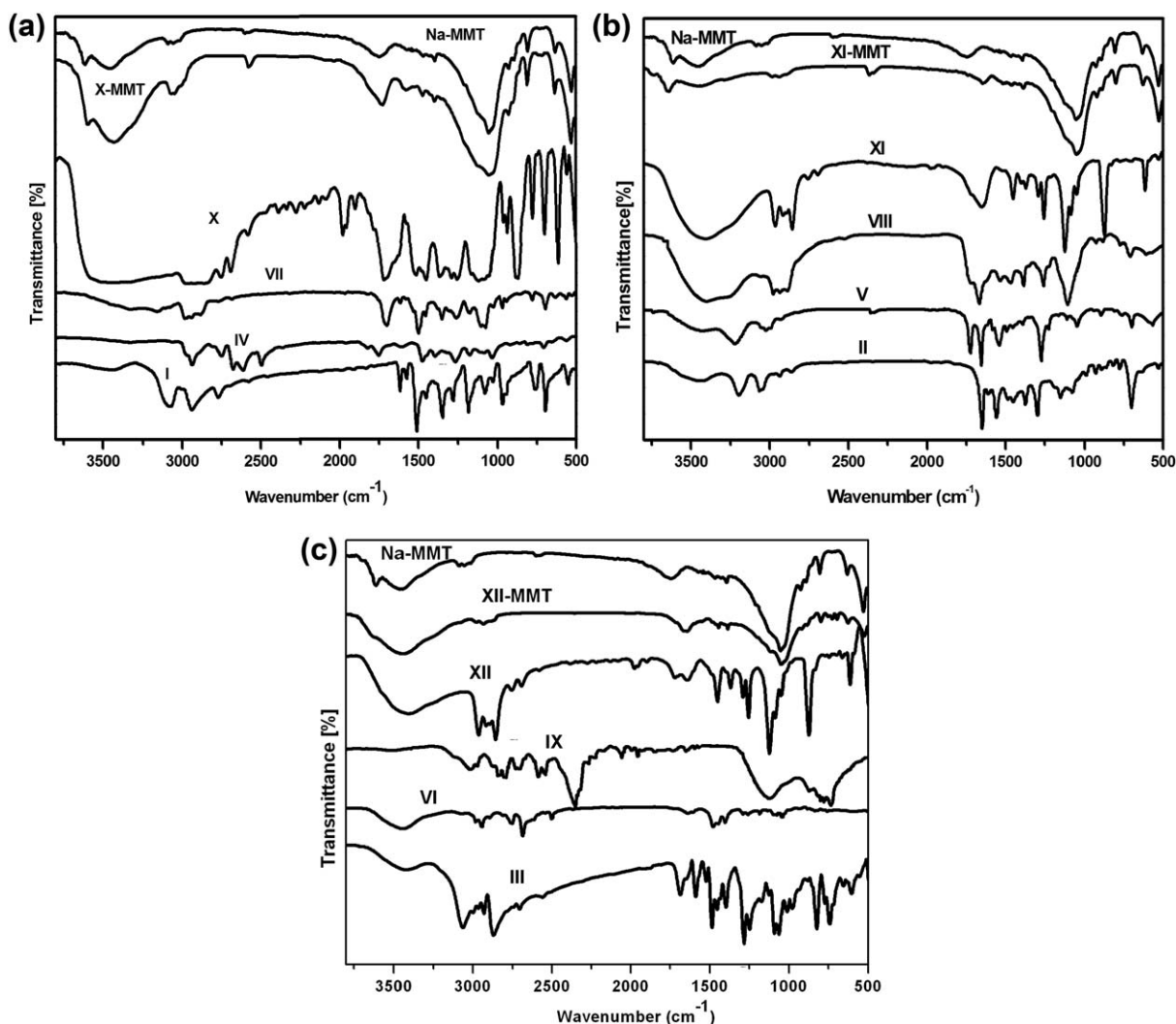


**Figure 1.** (a–c) FT-IR spectra of 1,3,4-oxa (thia)-diazoles (I, II, III); Na-MMT; polyamides and their nanocomposites.

## RESULTS AND DISCUSSION

### Preparation and Characterization of Polyamide-MMT Nanocomposites

In this work, A series of polyamide containing chemically bound 1,3,4-oxa (thia)diazoles have been prepared by reaction of 5-phenyl-1,3,4-oxadiazole-2-thiol, 5-phenyl-1,3,4-oxadiazole-2-amine and 5-(4-chlorophenyl)-1,3,4-thiadiazole-2-thiol with ethyl chloroformate followed by polycondensation with jeffamine T<sub>403</sub>. Modification of the ester group was carried out by the nucleophilic replacement of the methoxy group with NH<sub>2</sub> in jeffamine T<sub>403</sub>. All the synthesized compounds were confirmed by <sup>1</sup>H-NMR and elemental analysis. The <sup>1</sup>H-NMR spectral data was found to be in quite agreement with the proposed structures.

FT-IR spectra (Figure 1) of 5-phenyl-1,3,4-oxadiazole-2-thiol (I) showed the SH at 2571 cm<sup>-1</sup>; 2-amino-5-phenyl-1,3,4-oxadiazole (II) showed the NH<sub>2</sub> at 3338 cm<sup>-1</sup>. While, 5-(4-chlorophenyl)-1,3,4-thiadiazole-2-thiol (III) showed the SH group at 2530 cm<sup>-1</sup>. The FT-IR spectra of IV–VI showed the

carbonyl ester in the range 1631 to 1748 cm<sup>-1</sup>. The conversion of the ester group in IV, V, VI to the amides VII, VIII and IX was followed by FT-IR spectra which showed partial loss of C=O band of the ester at 1631 to 1748 cm<sup>-1</sup> and the appearance of the NH stretching at 3322 to 3409 cm<sup>-1</sup> and the C=O stretching of the amide at 1634 to 1697 cm<sup>-1</sup>. FT-IR [Figure 1(a–c)] of Na-MMT shows the characteristic absorption bands at 3442 cm<sup>-1</sup> due to –OH stretching band for absorbed water. The band at 3632 cm<sup>-1</sup> is due to –OH band stretch for Al–OH. The overlaid absorption peak at 1639 cm<sup>-1</sup> is attributed to –OH bending mode of absorbed water. The characteristic peaks at 1199 cm<sup>-1</sup> and 1047 cm<sup>-1</sup> is due to Si–O stretching (out of plane) and Si–O stretching (in-plane) vibration for layered silicate, respectively. Peaks at 918 cm<sup>-1</sup>, 883 cm<sup>-1</sup>, and 797 cm<sup>-1</sup> are attributed to AlAlOH, AlFeOH, and AlMgOH bending vibrations, respectively. FT-IR is an appropriate technique to study polymer-clay interaction. Comparing bands in polymer amine hydrochloride (X–XII) and the corresponding composites (X-MMT, XI-MMT, XII-MMT) a shift from 1642 to 1719 cm<sup>-1</sup> was reported giving an indication that NH<sub>3</sub><sup>+</sup> was electrostatic

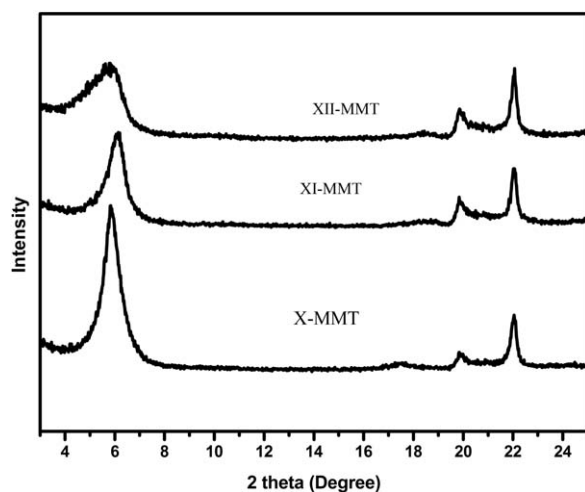


**Figure 2.** X-ray diffraction pattern of polyamide-MMT nanocomposites.

intercalated to more negative site  $^-$ O-MMT. The shift to higher wave number indicates that the interaction between polymers and negatively charged clay occurs through ionic interaction

between  $\text{NH}_3^+$  and MMT. It was reported that there is a shift in N-H vibration due to chelation of transition metal ions by  $\text{NH}_2$  group.<sup>48</sup>

Figure 2 shows the XRD pattern of nanocomposites. The characteristic  $2\theta$  peaks of 001 plane for X-MMT, XI-MMT, and XII-MMT are observed at  $5.84^\circ$ ,  $5.8^\circ$ ,  $6.14^\circ$  with basal spacing of 15.15, 15.23, and 14.38 Å. According to the Bragg's law, the peak shifting from lower  $d$ -spacing (9.6 Å) characteristic to Na-MMT to higher one is due to the intercalation of polymer into the interlayer of MMT. XRD is unable to detect regular stacking exceeding 88 Å. One may note that the commonly used definition of an exfoliated nanocomposite is based on layer spacing larger than this value. In reality, it was the transmission electron microscopic analysis that evidenced the formation of nanocomposite.

More direct evidence for the formation of a nanocomposite is provided by the TEM of film produced from cast suspension of nanocomposite in acetone. TEM images of X-MMT, XI-MMT, and XII-MMT [Figure 3(a–c)] display individual silicate layers appear as dark lines. There are some irregular dispersions of the

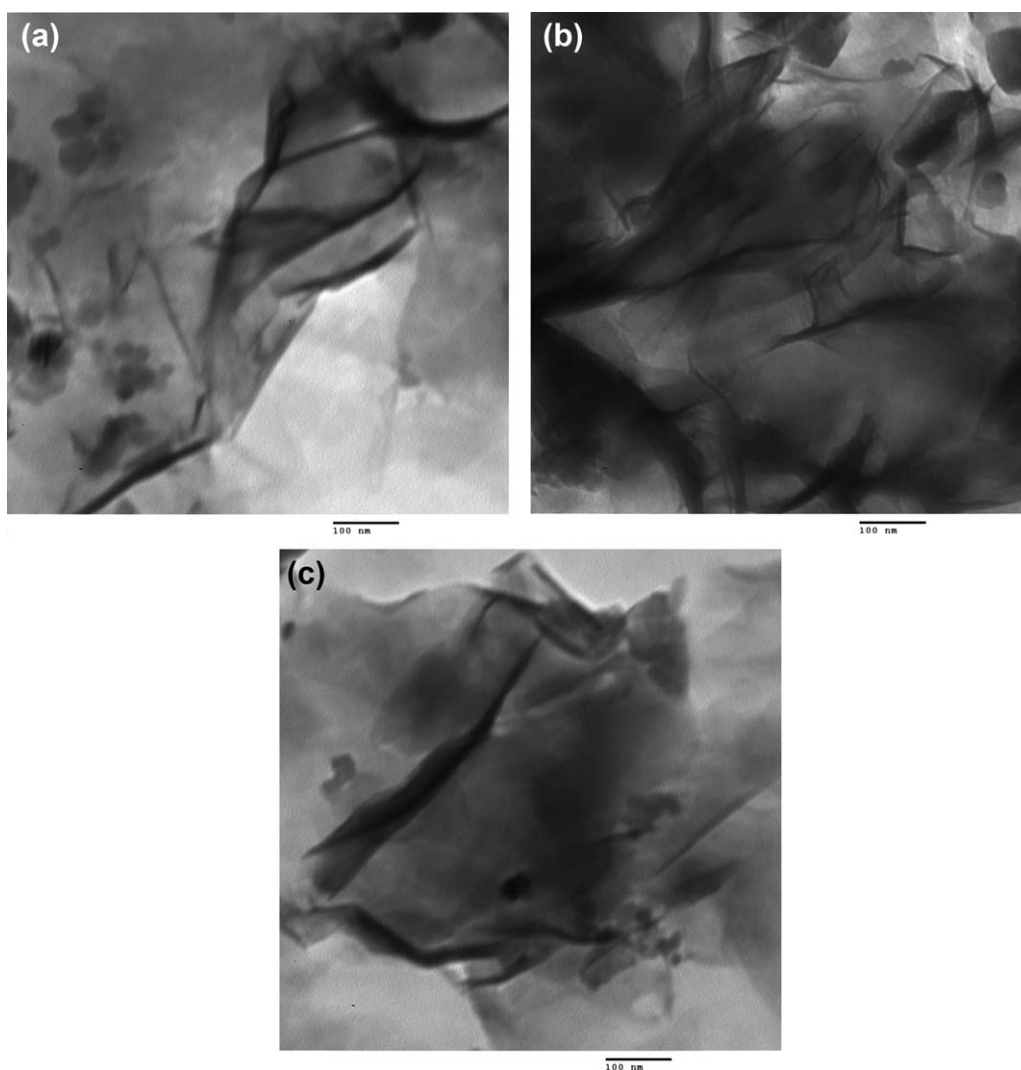


**Figure 3.** Transmission electron micrograph of a) X-MMT; b) XI-MMT; c) XII-MMT.



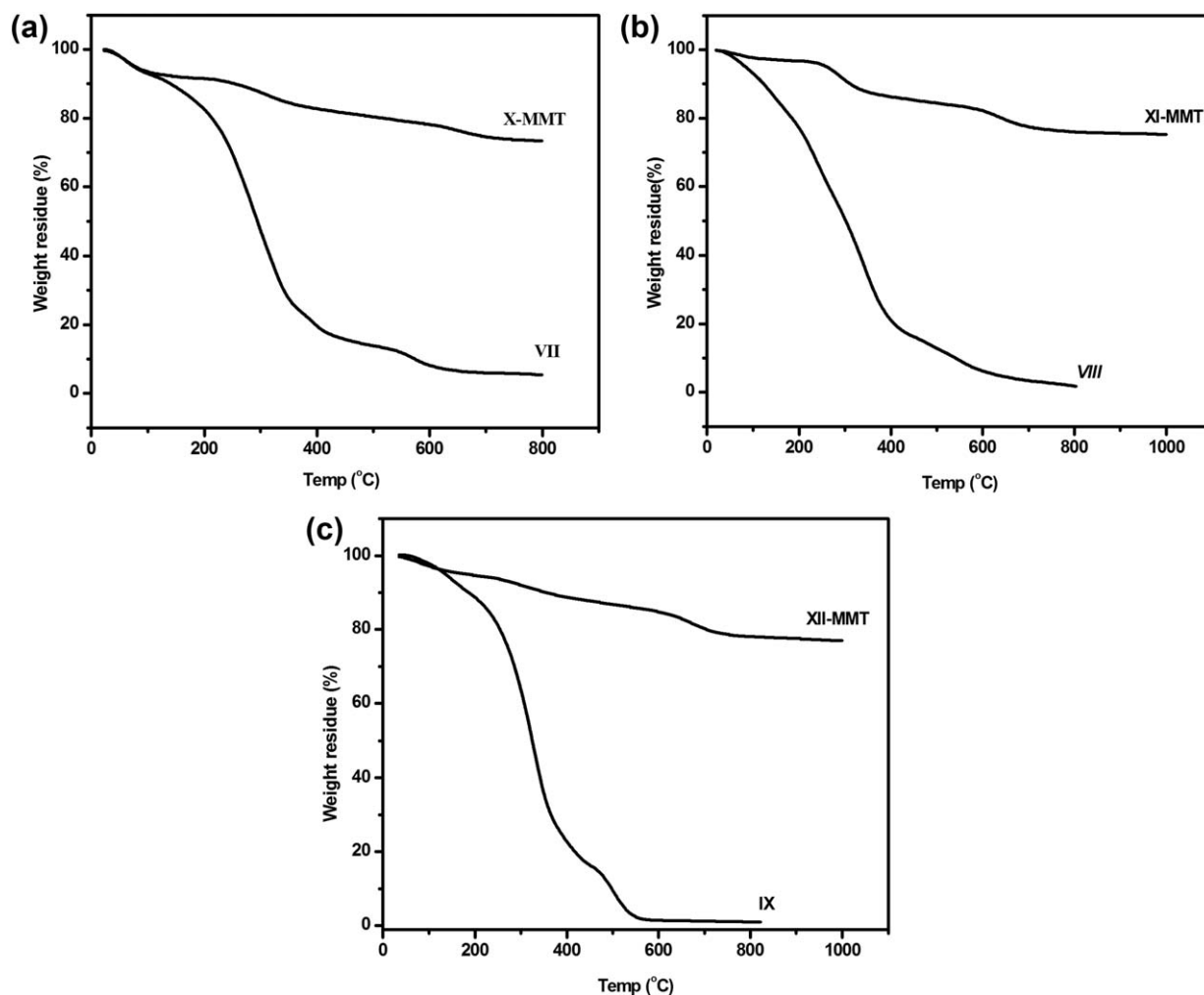


**Figure 4.** (a-c) TGA thermograms of polyamides (VII, VIII, IX) and their nanocomposites (X-MMT, XI-MMT, XII-MMT).

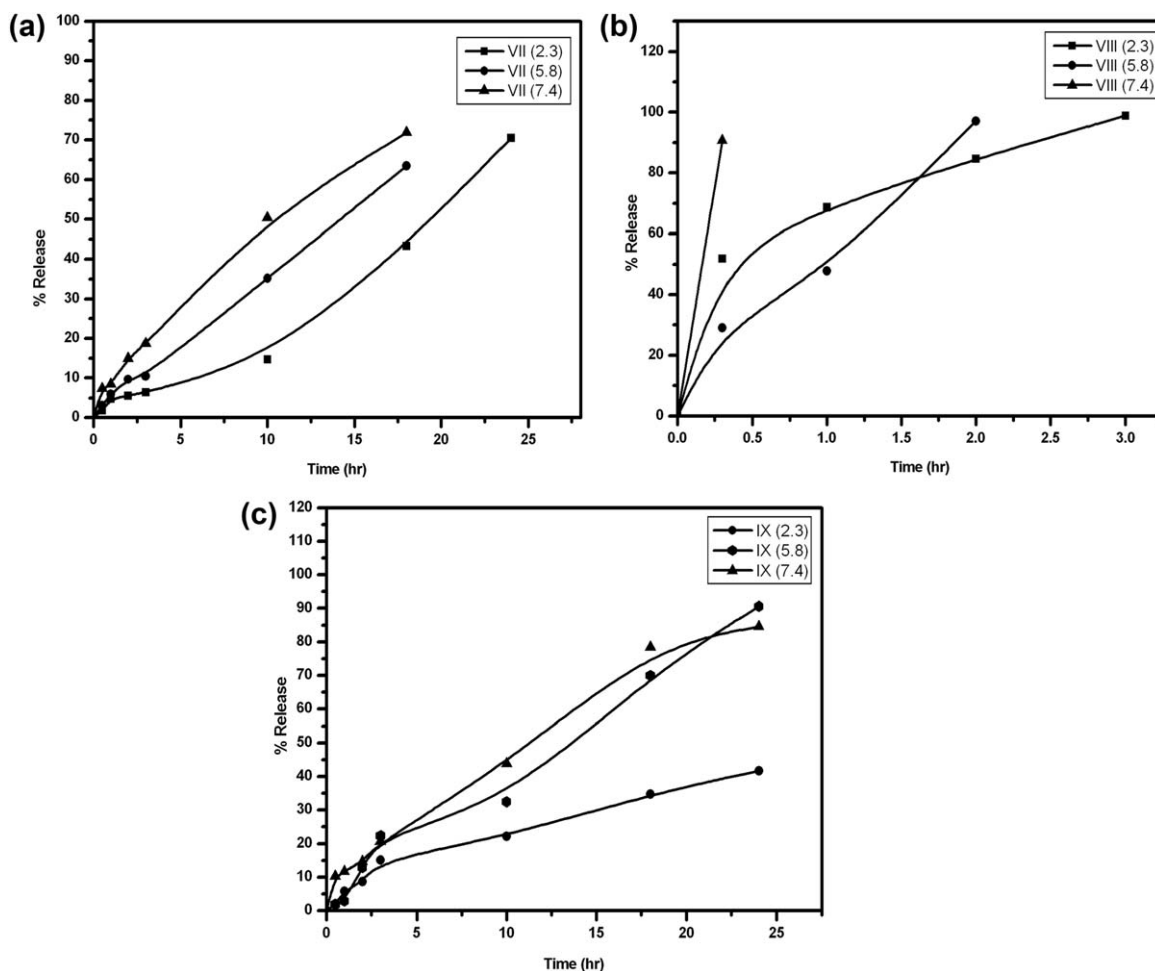
silicate layer in X-MMT and XII-MMT. Some particles maintained their original ordering while others were exfoliated. This is consistent with the observation of XRD studies shown in Figure 2. However, TEM image of XI-MMT indicates that the separation between the dispersed plates is higher than in X-MMT and XII-MMT nanocomposites. This TEM photograph proves that the most clay layers were exfoliated and dispersed homogeneously into polyamide matrix. Considering the proceeding results, the existing morphology could be affecting the release behavior of heterocyclic compounds.

Figure 4 depicts the TGA for VII, VIII, and IX and their nanocomposites. It was reported that<sup>49</sup> two major weight loss patterns were observed in the temperature range of 80–100°C and 600–750°C for Na-MMT. The first weight loss corresponds to evaporation of absorbed water. The second prominent weight loss was observed at 600 to 750°C due to the loss of structural hydroxyl group. VII, VIII and IX shows a sharp weight loss at around 200 to 400°C. However, X-MMT, XI-MMT, and XII-MMT nanocomposites shows weight loss in three steps in the temperature range 60 to 100°C, 300 to 400°C, and 600 to 750°C. It is explained that decomposition of intercalated poly-

mer took place in the temperature range of 300 to 350°C. A weight loss at 100°C and 650°C is due to loss of water and structural hydroxyl group in the nanocomposites, respectively. In addition, the thermal degradation patterns from TGA have evidenced the presence of the polymer in the MMT interlayer confinement. Considering the above results, it is consistently believable that the introduction of inorganic components into organic polymers can improve their thermal stability on the basis of the fact that clay has good barrier and thermal properties.<sup>31,50,51</sup>

#### Release Profiles

One of the problems in biomaterials for drug delivery and need to overcome is the burst release of encapsulated or entrapped drugs. By controlling the release of drugs, one can not only optimize the therapeutic effects of the drug, but also influence their biological activity. The controlled release tests were carried out by suspending the polyamide (VII, VIII, and IX) and their nanocomposites (X-MMT, XI-MMT, and XII-MMT) in the buffer solution at pH 2.3, 5.8, and 7.4. The amount of heterocyclic compounds (I, II and III) released from polyamide (VII, VIII, and IX) was measured at 2880 min of time intervals by



**Figure 5.** *In vitro* release 1,3,4-oxa (thia)-diazoles (I, II, III) from polyamides (VII, VIII, IX) polyamides at different pH (2.3, 5.8, 7.4).

measuring the absorbance at  $\lambda_{\max} = 343$  nm,  $\lambda_{\max} = 301$  nm and  $\lambda_{\max} = 248$  nm, respectively. The results (Figure 5) showed that the release behavior depends on the pH of the medium in the order  $7.4 > 5.8 > 2.3$ ; 50% of I was released after 10 hr, 15 hr, and 19 hr at pH 7.4, 5.8, and 2.3, respectively. The release of II reaches 90% after 30 min, 1.5 hr, 2 hr at pH 7.4, 5.8, and 2.3. The release of III reaches 90% at pHs 5.8 and 7.4 after 24 hr and 40% after 25 hr at pH 2.3. In the slightly basic medium, the hydrolysis of the amide linkages takes place through the attack of the nucleophile on the electron-deficient carbonyl. Figure 6 shows the release of I, II, and III from X-MMT, XI-MMT, and XII-MMT at different pH. Comparing release of 1,3,4-oxa(thia)-diazoles (I, II, III) from polyamides and intercalated nanocomposites of the same polymer presented in Figure 6 shows that linear polymers were characterized by faster rates than the intercalated polymers. The increase in the rates was attributed to higher interactions of polymers with the used medium than the intercalated polymers. Also the higher content of 1,3,4-oxa(thia)-diazoles in linear polyamides leads to increase the rate of release. This slow release process may be interpreted based on the good barrier properties<sup>31</sup> due to the tortuous diffusion pathways that small molecules must travel in order to clear the material. This explained that nanocomposite formation resulted

in sustained release of heterocyclic compounds in comparison with the polymer. Figure 6 revealed that 10%, 32% and 16% of I, II, and III was released after 24 hr, respectively at pH 2.3. A comparison between the release rates from X-MMT, XI-MMT, XII-MMT suggest that the rate increases with increasing the hydrophilic characters of polyamides loaded 1,3,4-(oxa)diazoles. Presence of NH—CO—NH in XI-MMT increases the surface area in contact with the hydrolyzing medium than X-MMT, XII-MMT that contains S—CO—NH group. It was reported that nanocomposites based on poly(ethylene vinyl acetate) (EVAc) and three different organo silicates (one montmorillonite and two synthetic micas), provided slow release of dexamethasone (a corticosteroid agent widely used to reduce inflammatory disease) as well as enhanced mechanical properties in comparison with the free polymer.<sup>52</sup>

#### Antimicrobial Activity

All the synthesized compounds were screened for their antimicrobial activity. The obtained results illustrated in Figure 7 and Table I showed that I, II, III, VII, VIII, and IX had a significant antimicrobial activity against tested microorganisms with variable inhibition zones expressed as mm. The highest antimicrobial activity of compound III than I and II may be related to

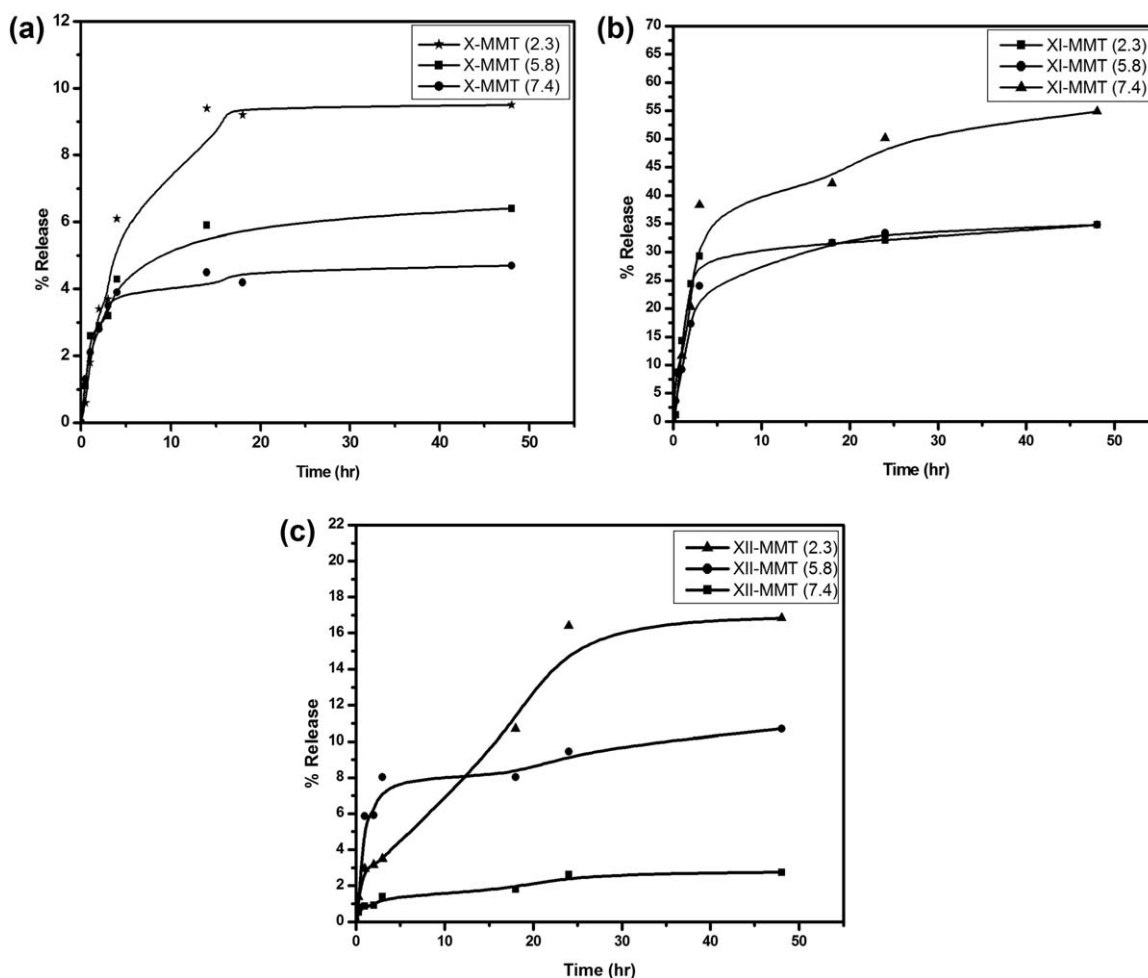


**Figure 6.** *In vitro* release of 1,3,4-oxa(thia)-diazoles (I, II, III) from a) X-MMT; b) XI-MMT; c) XII-MMT polyamide-MMT nanocomposites at different pH(2.3, 5.8, 7.4).

**Table I.** Inhibition Zones (mm) of Tested Compounds Against Different Microorganisms

Tested compounds	Inhibition zone (mm)/tested microorganisms						
	<i>B. subtilis</i>	<i>Shegilla sp</i>	<i>A. hydrophila</i>	<i>S. aureus</i>	<i>E. coli</i>	<i>C. albicans</i>	<i>A. niger</i>
I	13.4 ± 0.03	11.5 ± 0.05	17.2 ± ±0.23	16.2 ± 0.03	14.3 ± 0.08	14.7 ± 0.06	13.7 ± 0.03
VII	16.7 ± 0.03	22.7 ± 0.18	19.8 ± ±0.03	22.00 ± 0.05	18.20 ± 0.23	17.80 ± 0.03	28.00 ± 0.05
X-MMT	0.00	0.00	0.00	0.00	0.00	0.00	0.00
II	0.00	18.30 ± 0.08	0.00	11.30 ± 0.06	12.30 ± 0.10	0.00	10.60 ± 0.06
VIII	24.30 ± 0.33	19.20 ± 0.08	19.50 ± 0.05	20.80 ± 0.14	15.70 ± 0.10	9.70 ± 0.12	19.50 ± 0.05
XI-MMT	0.00	0.00	0.00	0.00	0.00	0.00	0.00
III	20.80 ± 0.03	15.70 ± 0.19	26.30 ± 0.19	19.20 ± 0.08	19.70 ± 0.10	19.70 ± 0.06	16.50 ± 0.05
IX	23.80 ± 0.10	23.00 ± 0.00	26.20 ± 0.10	20.5 ± 0.05	25.20 ± 0.03	24.20 ± 0.10	38.30 ± 0.03
XII-MMT	0.00	0.00	0.00	0.00	0.00	0.00	0.00
ANOVA							
F	260.86	322.05	377.00	711.81	270.61	826.64	3939.38
P	0.00	0.00	0.00	0.00	0.00	0.00	0.00

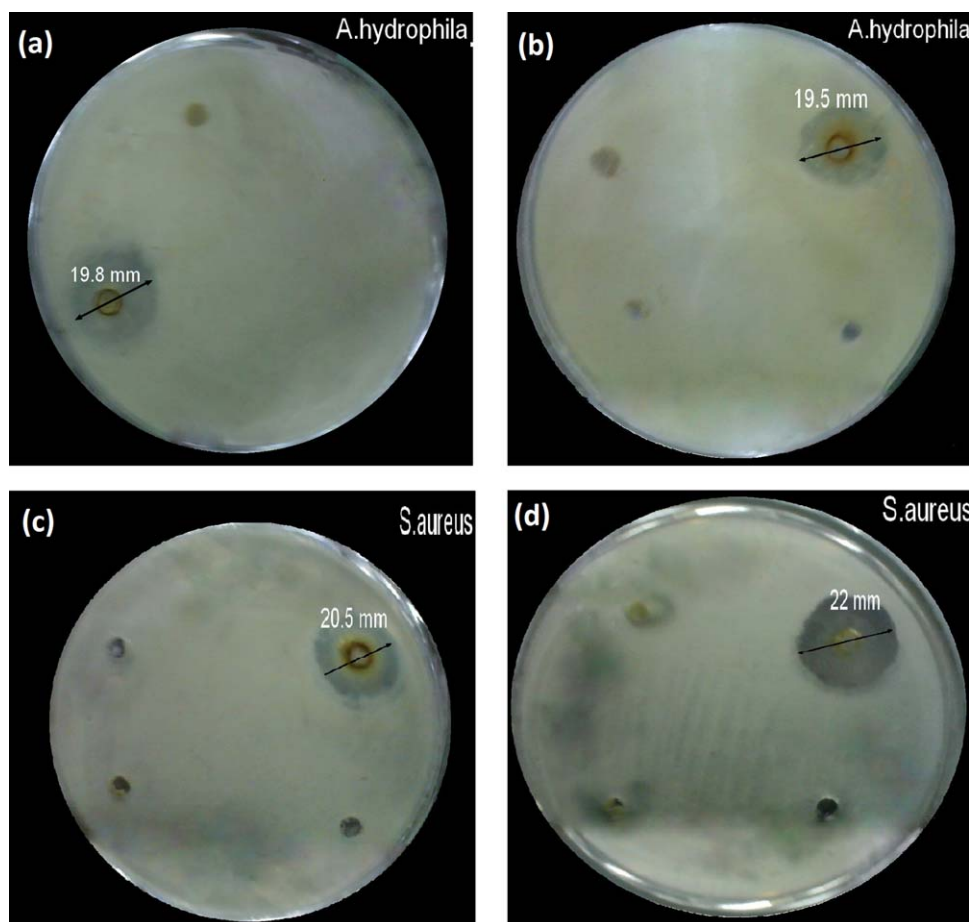


**Figure 7.** inhibition zones of (a) VII for *A. hydrophila* (b) VIII for *A. hydrophila* (c) IX for *S. aureus*, (d) VII for *S. aureus*. [Color figure can be viewed in the online issue, which is available at [wileyonlinelibrary.com](http://wileyonlinelibrary.com).]

the presence of two sulfur atoms in the molecule, one inside the hetero ring and the other as amidothio besides the presence of electron withdrawing (chlorine atom). It is interesting to note that a minor change in the molecular structure of investigated compounds may have a pronounced effect on antimicrobial screening. It was reported that methylene bridged benzisoxazolyimidazo [2,1-*b*][1,3,4]-thiadiazoles showed moderate to good bacterial inhibition.<sup>53</sup> It is worth mention that polyamides loaded 1,3,4-(oxa)diazoles (VII, VIII, IX) were more active against tested microorganisms than 1,3,4-(oxa)diazoles (I, II, III). This may be explained by the presence of  $\text{NH}_2$  and amide groups that affect the tested microorganisms. However, the results clearly revealed that the intercalation of polymers into clay (X-MMT, XI-MMT, XII-MMT) exhibit no *in vitro* antimicrobial activity against all tested microorganism. This may be attributed to the good barrier of clay<sup>31</sup> that decreases the contact between the functional groups and the tested microorganisms in this media. The most potent antimicrobial compounds were investigated to detect their MIC. Different concentrations of the most active antimicrobial compounds (VII and IX) were screened to detect their MICs and MBCs values against *A. hydrophila* (the most sensitive one). The obtained results showed that the MIC and MBC values of VII and IX were recorded at 12.5 and 25 mg/mL (MICs) and were 6.25 and

3.16 mg/mL (MBCs), respectively. However, tetracycline which used as a standard antimicrobial drug needed lower concentration (0.012 and 0.0062 mg/mL) to give the same effect.

Statistical analysis (Table I) showed that the effect of the tested compounds on the tested organisms were highly significant at probability value ( $P < 0.01$ ) on diameters of inhibition zones.

#### Antimicrobial, Toxicity, and Anti-Inflammatory Properties in Experimental Animals

The preliminary results presented in *in vitro* study suggested that VII, IX may offer good antimicrobial activity. Infection was induced by topical application of the bacteria into burn site on the animal's backs and treated with the same manner. The ability of tested compounds (VII, X-MMT, IX, and XII-MMT) to inhibit the spread of bacteria from infected burn wound to other organs were compared to untreated control and Mebo treated groups. The results in Table II show that the number of bacteria in blood increased after two days than in organs due to its transport from skin to blood. All tested compounds revealed significant antimicrobial activities as they reduced *S. aureus* load in blood comparing to Mebo and control treatments. The number of bacteria was decreased with increasing the time post infection. This indicated the ability of investigated treatment to prevent or reduce sepsis.



**Table II.** Number of Bacterial Load in Blood and Organs (Skin, Spleen, and Liver) After Different Days

Code	Skin			Blood		
	2 Days	4 Days	6 days	2 Days	4 Days	6 Days
Control	181	193	210	214.50 ± 2.12	333.00 ± 94.75	449.50 ± 23.33
Na-MMT	150	172	189	132.50 ± 0.71	166.00 ± 0.00	216.50 ± 23.33
Mebo	135	165	200	183.00 ± 24.04	233.00 ± 0.00	350.00 ± 0.00
VII	100	50	30	169.50 ± 4.95	47.00 ± 4.24	0.00 ± 0.00
X-MMT	95	45	32	170.50 ± 6.36	28.00 ± 7.07	0.00 ± 0.00
IX	60	33	15	116.50 ± 4.95	13.00 ± 4.24	0.00 ± 0.00
XII-MMT	70	40	12	169.50 ± 19.09	45.00 ± 7.07	0.00 ± 7.07

	Spleen			Liver		
	2 Days	4 Days	6 Days	2 Days	4 Days	6 Days
Control	169.50 ± 4.95	258.00 ± 11.31	316.50 ± 23.33	200.00 ± 141.42	358.00 ± 35.36	449.50 ± 23.33
Na-MMT	165.00 ± 2.83	179.50 ± 4.95	231.50 ± 2.12	134.00 ± 1.41	175.00 ± 35.36	299.50 ± 47.38
Mebo	167.00 ± 1.41	185.00 ± 11.31	249.50 ± 23.33	136.50 ± 23.33	166.50 ± 47.38	383.00 ± 24.04
VII	166.50 ± 23.33	90.00 ± 56.57	30.00 ± 4.24	150.00 ± 212.13	66.00 ± 0.00	0.00 ± 0.00
X-MMT	158.00 ± 59.40	144.50 ± 40.31	66.00 ± 0.00	146.50 ± 4.95	38.50 ± 7.78	0.00 ± 0.00
IX	151.50 ± 2.12	66.00 ± 0.00	21.50 ± 12.02	183.00 ± 70.71	75.00 ± 35.36	49.50 ± 23.33
XII-MMT	101.50 ± 2.12	66.50 ± 23.33	28.00 ± 2.83	199.50 ± 23.33	58.00 ± 11.31	33.00 ± 0.00

The results revealed that compounds IX and XII-MMT had the highest reduction level of *S. aureus* on skin after 6 days of infection compared to that of untreated control group. The data reflect that compound VII and IX was the most effective treatment as it reduced bacterial load in spleen than other treatments. Treatments with X-MMT and XII-MMT showed moderate antibacterial activity when compared to Na-MMT, Mebo and control. VII and X-MMT possessed good antibacterial activity as they reduce bacterial load in liver when compared to other treatments.

#### Toxicity of Compounds on Shaved Mouse Healthy Skin

The mice in all treated and untreated groups did not show any sign of irritation (rash, inflammation, swelling, scaling, and abnormal tissue growth in the affected area) when observed for a period of seven days. In addition, wounds treated with IX and XII-MMT heal faster than untreated wounds. The results presented in this study suggested that VII, IX, X-MMT, and XII-MMT compounds may offer a promising and novel means for the treatment of *S. aureus* burn wound infection and open new insight into further investigation on this area. It is reported that<sup>54</sup> several 3,6-disubstituted-1,2,4-triazolo[3,4-b]-1,3,4-thiadiazoles and their dihydro analogues showed good anti-inflammatory.

#### CONCLUSION

We have shown the intercalation of polyamide loaded 1,3,4-oxa(thia)diazoles into MMT. The intercalation was achieved through an ion exchange process between sodium cations in Na-MMT and amine hydrochloride attached to the polyamides. XRD patterns show an increase in the d-spacing confirming the

intercalation of polyamides into the interlayer of MMT. FT-IR, TEM, and TGA have evidenced the presence of the polymer in the MMT interlayer confinement. The release study indicates that polyamide-MMT can be used as the sustained release of 1,3,4-oxa(thia)diazoles in oral administration. The polyamides showed good or moderate antimicrobial activities. *In vitro* studies of nanocomposites showed no antimicrobial effect. However, *in vivo* studies suggest that nanocomposites offer good antimicrobial activity.

#### REFERENCES

- Barbucenu, S. F.; Bancescu, G.; Cretu, O. D.; Draghici, C.; Bancescu, A.; Radu-Popescu, M. *Rev. Chem. (Bucuresti)* **2010**, *61*, 140.
- Kumar, G. V. S.; Rajendraprasad, Y.; Mallikarjuna, B. P.; Chandrashekar, S. M.; Kistayya, C. *Eur. J. Med. Chem.* **2010**, *45*, 2063.
- Shirote, P. J.; Bhatia, M. S. *Arab. J. Chem.* **2011**, *4*, 413.
- Parkash, O.; Kumar, M.; Sharma, C.; Aneja, K. R. *Eur. J. Med. Chem.* **2010**, *9*, 4252.
- Padmavathi, V.; Reddy, G. S.; Padmaja, A.; Kondaiah, P.; Shazia, A. *Eur. J. Med. Chem.* **2009**, *44*, 2106.
- Akhter, M.; Husain, A.; Azad, B.; Ajmal, M. *Eur. J. Med. Chem.* **2009**, *44*, 2372.
- Idrees, G. A.; Aly, O. M.; El-Din, G.; Abuo-Rahma, A. A.; Shazia, M. F. R. *Eur. J. Med. Chem.* **2009**, *44*, 3973.
- Jayashankar, B.; Rai, K. M. L.; Baskaran, N.; Shazia, H. S. S. *Eur. J. Med. Chem.* **2009**, *44*, 3898.

9. Kumar, D.; Sundaree, S.; Johnson, E. O.; Shah, K. *Bioorg. Med. Chem. Lett.* **2009**, *19*, 4492.
10. Shashikan, D.; Bhandari, V.; Bothara, K. G.; Raut, M. K.; Patil, A. A.; Sarkate, A. P.; Mokale, V. J. *Bioorg. Med. Chem. Lett.* **2008**, *16*, 1822.
11. Ikada, Y.; Tsuji, T. *Macromol. Rapid Commun.* **2000**, *21*, 117.
12. Jagur-Grodzinski, J. *Polym. Adv. Technol.* **2006**, *17*, 395.
13. Wan, Y.; Fang, Y.; Hu, Z.; Wu, Q. *Macromol. Rapid Commun.* **2006**, *27*, 948.
14. Ha, C.-S.; Gardella, J. A. *Chem. Rev.* **2005**, *105*, 4205.
15. Madan, P. L.; Chareonboonsit, P. *Pharm. Res.* **1989**, *8*, 714.
16. Makino, K.; Mack, E. J.; Okano, T.; Wan Kim, S. *J. Controlled Release.* **1990**, *12*, 235.
17. Ostad, S.; Farhadkhani, M.; Minaee, B.; Malihi, G.; Abdollahid, M. *DARU.* **2002**, *10*, 5.
18. Maheshwari, K. R.; Sharma, N. S.; Jain, K. N. *Indian Pharmacol. Sci.* **1988**, *50*, 101.
19. Joshi, G. V.; Kevadiya, B. D.; Patel, H. A.; Bajaj, H. C.; Jasra, R. V. *Int. J. Pharma.* **2009**, *374*, 53.
20. Aguzzi, C.; Cerezo, P.; Viseras, C.; Caramella, C. *Appl. Clay Sci.* **2007**, *36*, 22.
21. Lin, F. H.; Lee, Y. H.; Jian, C. H.; Wong, J. M.; Shieh, M. J.; Wang, C. Y. *Biomaterials* **2002**, *23*, 1981.
22. Zheng, J. P.; Luan, L.; Wang, H. Y.; Xi, L. F.; Yao, K. D. *Appl. Clay Sci.* **2007**, *36*, 297.
23. Fejer, I.; Kata, M.; Eros, I.; Berkesi, O.; Dekani, I. *Colloid Polym. Sci.* **2001**, *279*, 1177.
24. Wang, N.; Li, B.; Li, H.; Feng, J. *Geo. J. Chin. Univ.* **2000**, *6*, 306.
25. Hu, F.; Zheng, Z. L. *Shanxi Build Mater. J.* **2000**, *1*, 32.
26. Hu, F.; Zheng, Z. L. *Multi Purpose Utiliz. Miner. Resour.* **2000**, *4*, 28.
27. Chang, J. H.; Ana, Y. U.; Choa, D.; Giannelis, E. P. *Polymer* **2003**, *44*, 3715.
28. Cypes, S. H.; Saltzman, W.; Giannelis, M.E.P. *J. Controlled Release* **2003**, *90*, 163.
29. Kiersnowski, A.; Piglowski, J.; *Eur. Polym. J.* **2004**, *40*, 1199.
30. Lee, W. F.; Chen, Y. C. *J. Appl. Polym. Sci.* **2004**, *91*, 2934.
31. Salahuddin, N.; Abo-El-Enein, S. A.; Selim, A.; Salah-el-dien, O. *Polym. Adv. Technol.* **2010**, *21*, 533.
32. Puttipipatkjachorn, S.; Pongjan-Yakul, T.; Priprem, A. *Int. J. Pharmacol.* **2005**, *293*, 51.
33. Lee, W.-F.; Fu, Yao-Tsung J. *Appl. Polym. Sci.* **2003**, *89*, 3652.
34. Meng, N.; Zhou, N. L.; Zhang, S. Q.; Shen, J. *J. Appl. Clay Sci.* **2009**, *42*, 667.
35. Salahuddin, N.; Kenway, E. R.; Abdeen, R. *J. Appl. Polym. Sci.* **2012**, *125*, 157.
36. Salahuddin, N.; Badr, B.; Abdeen, R. *Polym. Compos.* **2012**, *33*, 643.
37. Salahuddin, N.; Badr, B.; Abdeen, R. *Polym. Int.* **2012**, *61*, 99.
38. Salahuddin, N.; Abdeen, R. *J. Inorg. Org. Met. Polymer.* **2013**, *23*, 1078.
39. Salahuddin, N.; Abdeen, R. *J. Modern Chem. Chem. Technol.* **2013**, *4*, 1.
40. Ainsworth, C. *Am. J. Chem. Soc.* **1956**, *78*, 4475.
41. Cipens, G.; Girnstains, V.; Kim, L. P. *SER.* **1962**, *2*, 255.
42. Potts, K. T.; Huse, R. M. *J. Org. Chem.* **1966**, *31*, 3528.
43. Muhi-Eldeen, Z.; Juma'a, G.; Al-Kaissi, E.; Nouri, L. *Jord. J. Chem.* **2008**, *3*, 233.
44. Mishra, A. R.; Rai, P.K.; Singh, C. R. *Ultra Chem.* **2012**, *8*, 211.
45. Delahaye, C.; Rainford, L.; Nicholson, A.; Mitchell, S.; Lindo, J.; Ahmad, M. *J. Med. Biol. Sci.* **2009**, *3*, 1.
46. Kumari, S.; Harjai, K.; Chhibber, S. *J. Infect. Dev. Countries* **2010**, *4*, 367.
47. Basketter, D. A.; York, M.; McFadden, J. P.; Robinson, M. K. *Contact Dermatitis* **2004**, *51*, 1.
48. Peppas, N. A.; Khare, A. R. *Adv. Drug Deliv. Rev.* **1993**, *11*, 1.
49. Hutchison, C. S. *Laboratory Handbook of Petrographic Techniques*; Mc Graw-Hill Book Co.: New York, **1973**.
50. Petrovic, Z. S.; Javin, I.; Waddong, A.; Banhegyi, G. *J. Appl. Polym. Sci.* **2000**, *76*, 133.
51. Messersmith, P. B.; Giannelis, E. P. *Polym. Chem.* **1995**, *33*, 1047.
52. Cypes, S. H.; Saltzman, W. M.; Giannelis, E. P. *J. Controlled Release* **2003**, *90*, 163.
53. Shetty, S. N.; Khazi, I. M.; Ahn, C. *Chem. Soc.* **2010**, *31*, 2337.
54. Mathew, V.; Keshavayya, J.; Vaidya, V. P.; Giles, D. *Eur. J. Med. Chem.* **2007**, *42*, 823.